



Published in final edited form as:

Arterioscler Thromb Vasc Biol. 2016 February ; 36(2): 370–379. doi:10.1161/ATVBAHA.115.306942.

The protein acyl transferase ZDHHC21 modulates α 1 adrenergic receptor function and regulates hemodynamics

Ethan P. Marin^{*}, Levente Jozsef^{*}, Annarita Di Lorenzo[†], Kara F. Held[†], Amelia K. Luciano[†], Jonathan Melendez^{*}, Leonard M. Milstone[‡], Heino Velazquez^{*}, and William C. Sessa[†]

^{*}Section of Nephrology, Yale School of Medicine, New Haven, CT 06520, USA

[‡]Department of Dermatology, Yale School of Medicine, New Haven, CT 06520 USA

[†]Department of Pharmacology and Vascular Biology and Therapeutics Program, Yale University School of Medicine, New Haven, CT 06520, USA

Abstract

Objective—Palmitoylation, the reversible addition of the lipid palmitate to a cysteine, can alter protein localization, stability, and function. The ZDHHC family of protein acyl transferases catalyzes palmitoylation of numerous proteins. The role of ZDHHC enzymes in intact tissue and *in vivo* is largely unknown. Herein, we characterize vascular functions in a mouse that expresses a nonfunctional ZDHHC21 (“F233”).

Approach and Results—Physiological studies of isolated aortae and mesenteric arteries from F233 mice revealed an unexpected defect in responsiveness to phenylephrine, an α 1 adrenergic receptor agonist. *In vivo*, F233 mice displayed a blunted response to infusion of phenylephrine and were found to have elevated catecholamine levels and elevated vascular α 1 adrenergic receptor gene expression. Telemetry studies showed that the F233 mice were tachycardic and hypotensive at baseline, consistent with diminished vascular tone. In biochemical studies, ZDHHC21 was shown to palmitoylate the α 1D adrenoceptor, and to interact with it in a molecular complex, thus suggesting a possible molecular mechanism by which the receptor can be regulated by ZDHHC21.

Conclusions—Together the data support a model in which ZDHHC21 F233 diminishes the function of vascular α 1 adrenergic receptors, leading to reduced vascular tone which manifests *in vivo* as hypotension and tachycardia. This is to our knowledge the first demonstration of a ZDHHC isoform affecting vascular function *in vivo* and identifies a novel molecular mode of regulation of vascular tone and blood pressure.

Keywords

palmitoylation; blood pressure; alpha adrenergic signaling

Correspondence: Dr. Ethan P. Marin, Section of Nephrology, Yale School of Medicine, 333 Cedar Street, PO Box 208029, New Haven, CT 06520-8029, Tel: 203-785-2178, Fax: 203-785-4904, ethan.marin@yale.edu.

Disclosures
None.

Introduction

The maintenance of vascular tone is of paramount importance to the health and survival of humans and other mammals. Multiple integrated signaling pathways coordinate to control vascular tone, which in turn determine blood flow distribution and blood pressure via alteration of peripheral vascular resistance. The $\alpha 1$ adrenergic receptor (AR) is a key determinant of vascular tone and its signaling has been the subject of intensive study over many decades. It is the target of several drugs that are used clinically to modify blood pressure¹. The identification of novel molecular pathways that may regulate $\alpha 1$ adrenergic signaling and blood pressure is of great importance in further developing our understanding of these critical pathways and in identifying novel drug targets.

Protein thioacylation is the post-translational attachment of a lipid, generally the saturated 16 carbon palmitate, to a cysteine sidechain via a labile thioester bond. Commonly referred to as palmitoylation, this modification typically affects the function of the substrate proteins by altering trafficking, localization, and/or stability². Unlike other lipid modifications such as prenylation or myristoylation, palmitoylation is reversible and thus may be regulated. Novel proteomic studies performed by us and others have shown that hundreds of cellular proteins in diverse tissues and cell types are palmitoylated and that palmitoylation can regulate cellular functions³⁻⁶.

The ZDHHC family includes more than 20 genes in mice and humans which encode enzymes that catalyze palmitoylation of substrate palmitoylproteins⁷. In yeast, knockdown of one or more ZDHHC isoforms attenuated palmitoylation of nearly all known palmitoylproteins, highlighting the importance of these enzymes in regulating cellular protein palmitoylation⁴. Historically, protein palmitoylation has been studied largely in biochemical or cellular assays. However, the recent identification of the ZDHHC family of proteins has allowed for *in vivo* studies on the role of protein palmitoylation via genetic approaches to alter enzyme expression and consequently modify cellular palmitoylprotein content. Several mouse models of ZDHHC deficiency have been generated to examine the function of this family of enzymes. For example, a mouse with a hypomorphic ZDHHC5 allele displayed evidence of defective hippocampal dependent learning⁸ while knockout of ZDHHC17⁹ and ZDHHC13¹⁰ each led to a phenotype that mimics Huntington's disease, a progressive neurodegenerative disorder. In addition, ZDHHC enzymes have been associated with human diseases such as schizophrenia¹¹ and certain cancers^{12, 13}.

ZDHHC21 is a protein acyl transferase known to be expressed in endothelial cells and elsewhere^{14, 15}. We have previously shown that in cultured endothelial cells ZDHHC21 supports the palmitoylation of important functional proteins including endothelial nitric oxide synthase (eNOS)¹⁵, which produces the pleiotropic gaseous second messenger nitric oxide, and PECAM1, a cell adhesion molecule that may play a role in angiogenesis and transendothelial cell migration³. Others have identified additional substrates for ZDHHC21 including sex steroid receptors¹⁶ and the nonreceptor tyrosine kinases Fyn¹⁷ and Lck¹⁸.

In the present work, we sought to characterize the role of ZDHHC21 in vascular function *in vivo*. We used the depilated mouse¹⁹ (MGI: 94884) which harbors a spontaneous mutation

in the gene for ZDHHC21. The resulting mutant protein has a deletion of phenylalanine 233 (“F233”) and lacks acyl transferase activity toward established substrates¹⁷. For example, ZDHHC21 F233 cannot palmitoylate eNOS nor Fyn in *in vitro* assays. Unexpectedly, we find that the F233 homozygous mice as well as derived cells and tissues display reduced responsiveness to α 1 adrenergic receptor (α 1AR) agonists. In vivo, tachycardia and hypotension were observed in the F233 mice, findings consistent with reduced peripheral vascular resistance as the result of impaired vascular action of α 1 AR. Molecularly, ZDHHC21 is found to form a complex with the α 1D AR, and increase its palmitoylation. These results suggest a molecular mechanism for the action of ZDHHC21, since palmitoylation has been shown to alter signaling and function of many related G protein coupled receptors. These data are to our knowledge the first demonstration of the *in vivo* role of a particular protein acyl transferase in vascular function and reveal a novel mode of regulation of vascular responsiveness to α 1 AR agonists. These data may pave the way to novel therapeutics that modulate vascular tone by altering protein acyl transferase activity.

Material and Methods

Materials and Methods are available in the online-only Data Supplement.

Results

Vessels isolated from F233 mice display impaired responsiveness to phenylephrine, an α 1 adrenergic receptor agonist

In order to evaluate vascular function in F233 mice, we studied aortic rings isolated from WT and mutant mice by wire myography (Fig. 1). When contraction was induced by phenylephrine, an α 1 adrenergic receptor (AR) agonist, maximal increases in tension were reduced by ~30% in F233 rings relative to WT (Fig. 1A; WT, 0.92 ± 0.08 g; F233, 0.64 ± 0.05 g; $p < 0.001$). $\text{Log}(\text{EC}_{50})$ for phenylephrine were similar (-7.0 ± 0.3 vs -6.9 ± 0.3). Contraction induced by a distinct receptor agonist, serotonin, was not impaired (Fig. 1B), nor was contraction induced by high concentrations of potassium, a receptor-independent stimulus (Fig. 1C).

In addition, endothelial-dependent relaxations were studied in response to acetylcholine. Regardless of whether vessels were precontracted with phenylephrine or serotonin, endothelial dependent relaxations were indistinguishable in WT and F233 mice (Supplemental Fig. 1).

Since the aorta is a conduit vessel and does not contribute significantly to peripheral vascular resistance *in vivo*, we sought to evaluate function of the mesenteric artery. Using pressure myography in cannulated vessels, we found that high concentrations of potassium in both WT and F233 third order mesenteric arteries induced similar contractions (not shown). However, as in the aortae, vessels derived from F233 mice displayed significantly reduced maximal contraction to phenylephrine (Fig. 1D; WT, 109 ± 7 %; F233, 49 ± 5 %, $P < 0.0001$). In addition, $\text{Log}(\text{EC}_{50})$ for phenylephrine in the mutant was similar to WT (WT, -5.9 ± 0.2 ; F233, -5.4 ± 0.3).

The above data suggest defective functioning of the α_1 AR in the vascular smooth muscle cells. We have previously demonstrated expression of ZDHHC21 using quantitative PCR (qPCR) approaches in cultured endothelial cells³, but expression has not been documented in vascular smooth muscle. We thus performed qPCR experiments on a variety of mouse tissues and cultured mouse cells (Suppl. Fig. 2). ZDHHC21 transcripts were confirmed in aorta, heart, as well as cultured mouse aortic smooth muscle cells. Overall, expression was noted in all tissues tested at fairly similar levels: the highest expressing tissue was only threefold higher than the lowest. Similar widespread expression of ZDHHC21 has been reported elsewhere¹⁴.

F233 mice display impaired response to infusion of phenylephrine

In order to determine whether the hyporesponsiveness to phenylephrine that was observed in isolated vessels was also present in intact mice, phenylephrine was infused into WT and F233 mice while blood pressure was monitored. Mice were maintained under inhaled isoflurane anesthesia while blood pressure was measured directly via a carotid artery catheter. Pre-infusion blood pressures were similar in WT and F233 mice under these conditions. Phenylephrine was infused at 30ug/kg/min for 15 min, and the steady state blood pressure was determined at the conclusion of the infusion period. As shown in Fig. 2, SBP increased substantially within 2–3 min following initiation of the phenylephrine infusion. At 15 min, the steady state SBP had increased by 15.6 \pm 1.8 mmHg in WT versus only 8.2 \pm 0.7 mmHg in F233 mice ($p=0.003$; $n=6$).

F233 mice display reduced blood pressure and tachycardia

The impaired response to α_1 AR agonists observed in isolated vessels and in intact mice suggest that F233 mice might exhibit evidence of diminished peripheral vascular resistance *in vivo*. In order to explore this possibility in awake, unrestrained mice, we used a telemetry system to characterize the hemodynamics of the F233 and WT mice. The averaged results from data collected continuously over 72h showed that all the mice displayed characteristic diurnal variations in blood pressure (BP) and heart rate (HR) (Fig. 3). The F233 mice were hypotensive, particularly at peak nighttime hours (Fig. 3A, Supplemental Table 1), which in nocturnal rodents is a period of increased activity, HR, and BP. Mean arterial pressure (MAP) at night was reduced in F233 mice relative to WT by 5.1 \pm 2.1 mmHg ($n=7$, $p=0.03$), but was not statistically different during the day (Fig. 3A, 3B; Supplemental Table 1).

The F233 consistently displayed increased HR relative to WT (Fig. 3G, H), however the pattern was opposite that of BP in that differences were greater during the day (66 \pm 20 beats/min, $p=0.007$) and smaller at night (49 \pm 19 beats/min, $p = 0.02$). The tachycardia was not the result of increased physical activity on the part of the F233 mice as measurements of activity collected using the telemetry system revealed that the F233 mice were less active at night than the WT mice (WT, 13.9 \pm 2.0 vs. F233, 5.2 \pm 0.4 arbitrary units, $p = 0.001$).

Further analysis of relationships between HR and BP suggest that the tachycardia in the F233 mice served to attenuate differences in blood pressure between the strains. For

example, the differences in blood pressure were smallest during the day, when greatest relative increase in HR in the F233 mice was observed (Fig. 3; Supplemental Table 1). At night, the differences in blood pressure were largest, and differences in HR were smallest. A plot of the difference in mean HR between WT and F233 versus the difference in MAP (Suppl Fig. 3A) suggests that MAP would be ~13 mmHg less in F233 mice if HRs were equivalent. The plot also reveals that when blood pressure was similar between the strains, the HR was ~70 bpm greater in the F233 mice. A plot of the same data set as mean HR vs. mean MAP for each strains clearly indicate the rightward shift of the curve in the F233 mice, illustrating the increased HR required to attain the same BP in this strain (Suppl Fig. 3B).

Variability in heart rate was assessed by determining the standard deviation of inter-beat intervals (SDIBI) in WT and F233 mice. This variability may increase with increased cholinergic input²⁰. Although the SDIBI was less in F233 mice, the difference was not statistically significant (WT, 6.5±1.5 msec; F233 4.7±1.0 msec; p= 0.32; Supplemental Table II).

F233 mice have elevated catecholamine levels and expression of α 1 AR

Since mutant mice and isolated arteries were found to be hyporesponsive to pharmacologic α 1 adrenergic agonist, we hypothesized that levels of endogenous expression of α 1 AR and its agonists might be altered in the mutant mice. In order to assess this possibility, we measured catecholamine levels in overnight urine collections (Fig. 4). Overnight collections reflect levels present when BP differences were greatest. Both adrenaline and noradrenaline levels were found to be significantly elevated in the F233 mice, suggesting increased average plasma levels during this time period. Further, qPCR analysis of aortae showed that mRNA levels for α 1A AR was significantly increased in mutant vessels, while subtypes 1B and 1D were not statistically different (Fig. 4C). In contrast, mRNA levels for contractile proteins, MYH11 and SMA2, were not significantly different in F233 as compared to WT.

F233 mice do not display evidence of cardiac abnormalities

The combination of hypotension and tachycardia seen in the F233 mice, while consistent with diminished vascular tone, might also be the result of cardiac dysfunction. In order to assess this possibility, we performed transthoracic echocardiography to examine cardiac structure and function. There were no significant differences in stroke volume, ejection fraction, or left ventricular volume at systole or diastole between WT and F233 mice (Table 1). Further, H+E stained sections of F233 myocardium did not reveal any obvious abnormalities (not shown). These data together suggest the hemodynamic phenotype does not relate to abnormal cardiac function.

F233 mice do not have evidence of abnormal fluid losses

The combination of tachycardia and hypotension might arise from a reduction in intravascular volume, which would contribute to reduced cardiac output by reducing preload. The normal stroke volume and left ventricular diastolic volume observed by echocardiography argues against this possibility (Table 1), but we nonetheless further evaluated fluid losses from skin and kidney. The F233 mice have abnormal skin

characterized by thickened epidermis and thinned coat raising the possibility of a defect in cutaneous barrier function, though none was detected in published investigations¹⁷. To confirm this, we directly measured trans-epidermal water losses in homozygous mutant and heterozygous control mice at age 4–6d, before the onset of hair growth which interferes with the measurements. The skin and fur of heterozygous mice are grossly indistinguishable from WT, thus water flux in the heterozygotes is expected to reflect that in the WT. In this assay, no significant difference between F233 and heterozygous mice was noted (Fig. 5).

In order to evaluate whether the F233 mice displayed abnormal handling of salt and water, serum analyses from mice on standard chow were performed (Table 2). They revealed no differences in blood urea nitrogen, sodium, nor potassium, suggesting no significant differences in renal function, renal handling of water and potassium, nor in the renin-angiotensin-aldosterone pathway. H+E stained sections of renal tissue did not reveal any obvious significant abnormalities in F233 mice (not shown). In order to further test for hemodynamically significant renal salt (and water) wasting, mice were placed on a very low salt diet (0.01%) while simultaneously monitoring hemodynamic status using a telemetry system. If the mutant mice were unable to appropriately retain sodium under conditions of dietary deprivation, they would be expected to demonstrate worsening tachycardia and hypotension associated with progressive fluid losses and intravascular depletion. However, both F233 and WT mice were able to tolerate the low sodium diet for two weeks with no discernible change in BP or HR (not shown). These data argue against significant salt wasting, but do not rule out a lowered “set point” for sodium retention under conditions of normal dietary intake.

Fibroblasts derived from F233 mice display reduced responses to phenylephrine

In order to further explore the mechanisms underlying the observed hyporesponsiveness to α_1 AR agonism in F233 mice, embryonic fibroblast cell lines were derived from WT and F233 mice. Signaling induced by phenylephrine was assessed by activation of the ERK1/2 pathway, a common pathway activated downstream of a variety of GPCRs. Signaling by F233 MEFs in response to phenylephrine (10 μ M) was markedly diminished (Fig. 6). At 5 min, the maximal increase in the ratio of phosphoERK to total ERK relative to time 0 was 2.5 \pm 0.3 for WT vs. 1.3 \pm 0.1 for F233, $p < 0.001$, $n = 7$). However, signaling by serotonin (10 μ M) was no different at 5 min (2.6 \pm 0.2 vs. 2.7 \pm 0.1, $p = \text{NS}$), mimicking the results observed with serotonin in isolated aortic rings. These results corroborate those obtained in intact aortic rings, and suggest that the molecular mechanism underlying this defect is preserved in cultured cells, and does not depend on the presence of differentiated smooth muscle cells nor of intact vascular tissue.

ZDHHC21 palmitoylates and interacts with α_1 AR *in vitro*

In order to examine the molecular basis of diminished α_1 AR function in F233 vessels, we hypothesized that ZDHHC21 may palmitoylate key proteins involved in the α_1 AR signaling pathway, and that loss of palmitoylation of those proteins might lead to disruption of α_1 AR signaling in the F233 mouse. Several proteins involved in canonical signaling by α_1 ARs are known to be palmitoylated. Most Class A G protein coupled receptors are palmitoylated at one or more cysteines in the C terminal tail distal to the seventh (i.e., last)

transmembrane helix, thus creating a “fourth” cytoplasmic loop²¹. Palmitoylation of the $\alpha 1B$ AR has been reported at such a position²². Further, $G_{\alpha q}$, the heterotrimeric G protein activated by $\alpha 1$ AR, is known to be palmitoylated, and to require palmitoylation for proper interaction with receptors^{22, 23}.

We tested for interactions between ZDHHC21 and $\alpha 1D$ AR and $G_{\alpha q}$ using a standard co-expression strategy²⁴ and biosynthetic incorporation of a palmitate analogue, 17-ODYA, into the palmitoylproteins⁶. ODYA can be derivatized with a fluorophore using click chemistry to allow for visualization and quantitation of protein palmitoylation.⁶ Since the $\alpha 1D$ subtype mediates vascular contraction in response to phenylephrine and catecholamines^{25, 26} we assessed whether $\alpha 1D$ AR was a substrate for ZDHHC21. As seen in Fig. 7A and quantified in 7B, palmitoylation of $\alpha 1D$ AR (myc tagged) was increased ~2.5 fold in the presence of WT ZDHHC21 (HA-tagged), but not when co-expressed with either ZDHHC21 F233 or a mutant in which the key catalytic cysteine is mutated to serine (C120S). Of note, $\alpha 1D$ AR was detected as 3 different bands, consistent with the presence of monomers, dimers and higher order aggregates. This multimerization of heterologously expressed $\alpha 1$ AR has been previously reported²⁷. Total expression of $\alpha 1D$ AR was increased by expression of WT, but not mutant ZDHHC21 (Fig 7A, 7B).

In addition to the receptor, the ability of ZDHHC21 to palmitoylate $G_{\alpha q}$ was tested, but no interaction was detected, in agreement with previously published results¹⁸. In contrast, both ZDHHC3 and ZDHHC7 increased $G_{\alpha q}$ palmitoylation, as previously reported¹⁸ (Fig. 7C and quantified in 7D).

As has been pointed out previously²⁸, a limitation of metabolic labeling studies in the assessment of palmitoylation is that it may reflect increased steady state palmitoylation, or merely increased turnover with either unchanged or even decreased steady state palmitoylation. In order to distinguish between these possibilities, we employed acyl-RAC methodology to purify palmitoylated receptors from cell lysates^{29, 30}. This label-free method purifies palmitoylated proteins from a mixture in the presence (but not absence) of hydroxylamine, and thus reflects the total pool of palmitoylated protein present. Using this analysis, we found that palmitoylation of $\alpha 1D$ AR was increased in the presence of ZDHHC21, albeit to a smaller degree than was observed using ODYA technique. These data suggest that ZDHHC21 does in fact increase steady state palmitoylation of $\alpha 1D$ AR, as well as total expression of $\alpha 1D$ AR. The smaller magnitude of the effect in this assay as compared with the ODYA technique is not unexpected, as it only distinguishes between protein that is not palmitoylated at all from that with at least one palmitoyl group. The addition of more palmitoyl groups beyond the first will not increase signal in the RAC assay, as it could in the ODYA/click experiment (Fig. 7A).

We additionally undertook analysis of $\alpha 1A$ and $\alpha 1B$ AR palmitoylation using ODYA labeling. However, extensive aggregation observed with these receptors precluded quantitative interpretation of the experiments (not shown). Aggregations seemed to be worse after immunoprecipitation, and exacerbated further by the click chemistry labeling reaction, perhaps due to the use of organic solvents in the reaction. We tried various detergent, buffer, and reducing conditions without satisfactory results. Experiments using the RAC technique

(which is less sensitive overall but less susceptible to aggregation due to use of SDS denaturation) failed to demonstrate increased palmitoylation of either $\alpha 1A$ or $\alpha 1B$ (Supplemental Fig. 4). These data do not rule out an interaction, but suggest that the effects on $\alpha 1D$ are the most robust.

As further evidence for interaction between $\alpha 1D$ AR and ZDHHC21 co-immunoprecipitation studies were performed. In several cases, ZDHHC enzymes have been found to co-immunoprecipitate with substrates^{15, 31}. Indeed, ZDHHC21 could be shown to co-immunoprecipitate with $\alpha 1D$ AR when co-expressed in HEK cells (Fig. 7G). Unfortunately, such experiments could not be performed on native tissues owing to lack of specific antibodies for $\alpha 1$ AR³². Together, these data suggest the ZDHHC21 could affect the function of $\alpha 1$ AR in VSMC by directly palmitoylating the $\alpha 1D$ receptor.

Discussion

This report documents the first demonstration that a particular ZDHHC palmitoyltransferase can regulate vascular function *in vivo*. Collectively, the data support a model (Fig. 8) in which inactivation of ZDHHC21 causes reduced responses to $\alpha 1$ AR agonists by diminishing palmitoylation of the $\alpha 1D$ AR, which manifests *in vivo* as diminished vascular tone (i.e. hypotension and tachycardia). Reduced responsiveness to phenylephrine was observed in intact mice (Fig. 2), isolated vessels (Fig. 1), as well as embryonic fibroblasts (Fig. 6). In contrast, responses to other stimuli for vascular contraction remained intact, such as serotonin and high $[K^+]$ in both isolated aortic rings (Fig. 1) and in MEFs (Fig 6), which suggests that the F233 vessels are not globally disabled. In further support of this model, in which disruption of vascular responsiveness to $\alpha 1$ AR plays a central role, we found increased levels of endogenous catecholamines and vascular $\alpha 1$ AR expression in F233 mice (Fig. 4).

The F233 mice were found to be hypotensive and tachycardic, which is consistent with diminished vascular tone. Diminished vascular tone is the expected phenotype in the setting of reduced $\alpha 1$ AR activity. Other explanations for the tachycardia and hypotension, such as cardiac abnormalities or loss of fluids via skin or kidney, were sought but not observed (Fig. 5, Table 1). Abnormalities of $\alpha 1$ AR function can clearly give rise to phenotypes similar to the one identified here for the ZDHHC21 mutant mouse. The most convincing data come from studies of $\alpha 1D$ KO mice, which display impaired phenylephrine induced contraction in aortic rings^{25, 33}, diminished pressor response to infused phenylephrine in intact mice²⁵, and hypotension^{25, 33, 34}. A separate study also found hypotension in $\alpha 1D$ KO mice relative to WT, but the difference (~3mm Hg) did not reach statistical significance³⁵. Further, two papers have shown that $\alpha 1D$ KO mice are resistant to the development of hypertension in a model employing salt loading and subtotal nephrectomy^{33, 35}.

The reduction in blood pressure in the F233 mice was relatively modest, in part due to masking by relative tachycardia (Suppl. Fig. 3). The tachycardia may be a “compensatory” response to the diminished vascular tone, but it could also result from other molecular defects not identified here, such as hyperactivity of the $\beta 1$ AR. The differences in blood pressure in F233 mice were largest, and statistically significant, only at night. This result

makes sense in light of our model which posits a role for diminished $\alpha 1$ AR pressor function, in that night is the time at which catecholamine levels are highest in rodents, and thus the time at which deficiency in $\alpha 1$ AR signaling would be expected to be most pronounced. A similar diurnal variation in blood pressure abnormalities was reported in the mouse knockout of TRIC-A, a monovalent cation channel. These mice displayed hypertension, but only during the daytime, as the high sympathetic output of nighttime hours masked the effect³⁶.

The Guytonian model of long term BP regulation would predict that in response to hypotension, the kidney would minimize sodium excretion so as to expand intravascular volume and normalize blood pressure³⁷. However, such renal compensation likely does not occur in the setting of vascular $\alpha 1$ AR dysfunction due to the involvement of the intrarenal vasculature in addition to other peripheral beds. Thus, renal blood flow is predicted to be preserved even at lower arterial blood pressures so that sodium retention is not triggered. Further, since $\alpha 1$ AR expressed in renal tubular epithelial cells may be involved in promoting renal tubular sodium reabsorption³⁸, its dysfunction may thwart the normal increase in tubular sodium reabsorption anticipated in the setting of hypotension. Regardless, the similarity of the phenotype between the F233 mice and several of the $\alpha 1$ AR KO mice suggests that defects in $\alpha 1$ AR are indeed sufficient to cause hypotension and tachycardia.

Regarding the molecular mechanisms underlying the defect in $\alpha 1$ AR signaling in the F233 mice, our results suggest that ZDHHC21 can directly interact with and palmitoylate the $\alpha 1D$ AR (Fig. 7), a subtype important for vasoconstriction in various vascular beds^{26, 39}. The palmitoylation of $\alpha 1D$ was specific, as ZDHHC21 could not palmitoylate G αq (Fig 7C). Palmitoylation of the $\alpha 1A$ and the $\alpha 1B$ receptors could not be demonstrated, though the data do not rule out an interaction (Suppl Fig 4). Unfortunately, direct demonstration of altered palmitoylation levels of $\alpha 1D$ receptors *in vivo* is technically quite difficult, owing to lack of availability of a suitable antibody³², and low receptor expression levels.

Numerous G protein coupled receptors have been found to be regulated in different ways by palmitoylation, which affects nearly all Family A receptors. Palmitoylation has been found in different studies to affect ligand binding, G protein coupling, and desensitization, though the details have varied depending on the particular receptor studied (reviewed in^{21, 40}). In addition, complexity related to GPCR palmitoylation and its functional role may arise from the fact that many GPCRs are palmitoylated at more than one site—and different sites may have different kinetics and play different functional roles, as was recently reported in the $\beta 1$ AR⁴¹. There are no previous reports regarding palmitoylation of $\alpha 1D$ AR, however, the $\alpha 1B$ AR was found to be palmitoylated at two cysteines in the C terminal tail in a ligand dependent fashion²². The significance of this palmitoylation was not determined and the catalytic enzymes(s) were not identified^{22, 23}.

Here, we find evidence that stability of $\alpha 1D$ AR are affected by palmitoylation, since co-expression of WT ZDHHC21 (but not the inactive mutants F233 or C120S) increased the expression levels (Fig 7B, 7F). An interrelationship between palmitoylation and protein

abundance has been observed in multiple proteins, and more recently was found to be a nearly universal phenomenon in proteomic analyses of hypomorph of ZDHHC5⁴² and hypomorph of ZDHHC17⁴³. In both cases, nearly all proteins found to be in less abundance after purification of palmitoylproteins were also found to be in less abundance in total pools. These results, using two unrelated systems, suggests that palmitoylation may commonly affect protein abundance and/or stability.

Investigations in the area of GPCR palmitoylation have nearly all been done in vitro, since creation of in vivo models of GPCRs that lack palmitoylation with traditional methods is difficult. Further, manipulation of GPCR palmitoylation via genetic alteration of ZDHHC enzyme expression has not been possible owing to lack of information on ZDHHC-substrate interactions, though recent data on GPCR palmitoylation has addressed this^{44,45}. In the one in vivo study on GPCR palmitoylation published, on the photoreceptor rhodopsin, a novel phenotype was discovered involving lack of stability of the unliganded opsin that is formed following bleaching of the receptor. Functionally, this instability caused retinal degeneration following exposure to bright light. This phenotype was not previously appreciated, despite multiple studies of rhodopsin palmitoylation that had been done in vitro. The F233 mouse thus represents an opportunity to explore the consequences of GPCR palmitoylation in vivo using genetic approaches.

Identifying substrates of ZDHHC enzymes that mediate in vivo phenotypes has been a difficult question^{42,43}. Although several mouse models of different ZDHHC isoform mutants, hypomorphs and knockouts have been reported, each with striking phenotypes ranging from neurodegeneration^{10,46} to osteoporosis⁴⁷, the identification of the exact molecular mechanism (i.e., the specific protein substrate in which lack of palmitoylation results in the observed phenotype) has been generally elusive. Broadly, investigators have tried unbiased proteomic approaches^{42,43} as well as more focused candidate gene approaches. The former has involved purification of palmitoyl proteins from tissues or cells of WT and mutant animals coupled with quantitative proteomic techniques. So far, relatively modest changes in the palmitoylome have been detected using these approaches, though a number of interesting candidates have been identified whose relevance to observed phenotypes awaits confirmation^{42,43}. Here, we used a candidate gene approach, which has the advantage of focusing on proteins with a known role in the observed phenotype. Further, this approach allows for direct investigation of proteins that may be too low in abundance to be readily detected with proteomic methods, such as GPCRs. A similar approach led to the identification of MT1-MMP as a possible substrate of ZDHHC13 that causes the osteoporosis that occurs in mice with a nonsense mutation in *Zdhhc13*⁴⁸.

Of course the candidate gene approach will not identify every substrate of a given ZDHHC enzyme, and available data suggest that most enzymes have multiple substrates⁴. For example, several additional substrates of ZDHHC21 have been reported, including eNOS, PECAM1, fyn⁴⁹, and sex steroid receptors¹⁶. It is likely that multiple proteins are differently palmitoylated in F233 mice besides α 1D AR. Thus the hemodynamic phenotypes described herein may not be (solely) due to nor fully explained by the identified interaction between ZDHHC21 and α 1D AR.

Of note, although previously published *in vitro* experiments had shown the knockdown of ZDHHC21 led to diminished palmitoylation of eNOS and reduced NO production⁵⁰, experiments with the F233 mice did not show any evidence of diminished eNOS function *in vivo*. For example, the mice were hypotensive (Fig. 3), not hypertensive as would be expected if eNOS function were diminished⁵¹. Further, endothelial function, as judged by acetylcholine-induced relaxations in isolated vessels (which depends on stimulated NO production), was normal (Supplemental Fig. 1). Thus, either the eNOS effects are overwhelmed by defective palmitoylation of other proteins, or eNOS is palmitoylated normally in the F233 mice, perhaps due to upregulation of other ZDHHC isoforms with reported activity toward eNOS⁵⁰.

In sum, this report shows for the first time that a ZDHHC protein acyl transferase enzyme, ZDHHC21, can affect vascular function *in vivo*, possibly by disrupting α 1 AR mediated vascular contraction. Several chemical inhibitors of both protein acyl transferases^{52, 53} and acyl protein thioesterases^{54, 55}, enzymes which catalyze palmitate removal, have been described. Thus, pharmacological manipulation of palmitoylation may soon be possible. ZDHHC21 and related family members may present novel targets for drug therapy to modulate vascular function.

Supplementary Material

Refer to Web version on PubMed Central for supplementary material.

Acknowledgments

We would like to thank Dr. Ian Smyth (Monash University, Australia) for sharing the depilated mice; Kerry Russell (Yale) for assistance with echocardiography; Jun Yu, Aldo Peixoto, Peter Aronson, Michael Caplan, Jordan Pober, Joseph Madri, and Lloyd Cantley (all of Yale) for helpful discussions; Nicole Mikush, Lonneta Diggs, and Roger Babbitt for technical assistance.

Sources of Funding:

This work was supported by: K08 HL103831, a pilot grant from the The George M. O'Brien Kidney Center at Yale, a Gottschalk Award from the American Society of Nephrology (to E.M.); R37 HL061371, R01 HL064793, R01 HL081190, and R01 HL096670 (to W.S.); T32HL007950 (K.H.); P30 DK079310 to support the George M. O'Brien Kidney Center at Yale.

Non-standard Abbreviations and acronyms

AR	adrenergic receptor
F233	mutant of ZDHHC21 protein in which phenylalanine 233 is deleted
ODYA	17-octadecynoic acid
5-HT	serotonin
SDIBI	standard deviation of inter-beat intervals

References

1. Sica DA. Alpha1-adrenergic blockers: Current usage considerations. *J Clin Hypertens (Greenwich)*. 2005; 7:757–762. [PubMed: 16330901]
2. Linder ME, Deschenes RJ. Palmitoylation: Policing protein stability and traffic. *Nat Rev Mol Cell Biol*. 2007; 8:74–84. [PubMed: 17183362]
3. Marin EP, Derakhshan B, Lam TT, Davalos A, Sessa WC. Endothelial cell palmitoylproteomic identifies novel lipid-modified targets and potential substrates for protein acyl transferases. *Circ Res*. 2012; 110:1336–1344. [PubMed: 22496122]
4. Roth AF, Wan J, Bailey AO, Sun B, Kuchar JA, Green WN, Phinney BS, Yates JR 3rd, Davis NG. Global analysis of protein palmitoylation in yeast. *Cell*. 2006; 125:1003–1013. [PubMed: 16751107]
5. Kang R, Wan J, Arstikaitis P, Takahashi H, Huang K, Bailey AO, Thompson JX, Roth AF, Drisdell RC, Mastro R, Green WN, Yates JR 3rd, Davis NG, El-Husseini A. Neural palmitoyl-proteomics reveals dynamic synaptic palmitoylation. *Nature*. 2008; 456:904–909. [PubMed: 19092927]
6. Martin BR, Cravatt BF. Large-scale profiling of protein palmitoylation in mammalian cells. *Nat Methods*. 2009; 6:135–138. [PubMed: 19137006]
7. Linder ME, Deschenes RJ. Model organisms lead the way to protein palmitoyltransferases. *J Cell Sci*. 2004; 117:521–526. [PubMed: 14730009]
8. Li Y, Hu J, Hofer K, Wong AM, Cooper JD, Birnbaum SG, Hammer RE, Hofmann SL. Dhhc5 interacts with pdz domain 3 of post-synaptic density-95 (psd-95) protein and plays a role in learning and memory. *J Biol Chem*. 2010; 285:13022–13031. [PubMed: 20178993]
9. Singaraja RR, Huang K, Sanders SS, Milnerwood AJ, Hines R, Lerch JP, Franciosi S, Drisdell RC, Vaid K, Young FB, Doty C, Wan J, Bissada N, Henkelman RM, Green WN, Davis NG, Raymond LA, Hayden MR. Altered palmitoylation and neuropathological deficits in mice lacking hip14. *Hum Mol Genet*. 2011; 20:3899–3909. [PubMed: 21775500]
10. Sutton LM, Sanders SS, Butland SL, Singaraja RR, Franciosi S, Southwell AL, Doty CN, Schmidt ME, Mui KK, Kovalik V, Young FB, Zhang W, Hayden MR. Hip14l-deficient mice develop neuropathological and behavioural features of huntington disease. *Hum Mol Genet*. 2013; 22:452–465. [PubMed: 23077216]
11. Young FB, Butland SL, Sanders SS, Sutton LM, Hayden MR. Putting proteins in their place: Palmitoylation in huntington disease and other neuropsychiatric diseases. *Prog Neurobiol*. 2012; 97:220–238. [PubMed: 22155432]
12. Yeste-Velasco M, Linder ME, Lu YJ. Protein s-palmitoylation and cancer. *Biochim Biophys Acta*. 2015; 1856:107–120. [PubMed: 26112306]
13. Greaves J, Chamberlain LH. New links between s-acylation and cancer. *J Pathol*. 2014;4–6. [PubMed: 24615251]
14. Ohno Y, Kihara A, Sano T, Igarashi Y. Intracellular localization and tissue-specific distribution of human and yeast dhhc cysteine-rich domain-containing proteins. *Biochim Biophys Acta*. 2006; 1761:474–483. [PubMed: 16647879]
15. Fernández-Hernando C, Fukata M, Bernatchez PN, Fukata Y, Lin MI, Bredt DS, Sessa WC. Identification of golgi-localized acyl transferases that palmitoylate and regulate endothelial nitric oxide synthase. *J Cell Biol*. 2006; 174:369–377. [PubMed: 16864653]
16. Pedram A, Razandi M, Deschenes RJ, Levin ER. Dhhc-7 and 21 are palmitoylacyltransferases for sex steroid receptors. *Mol Biol Cell*. 2011;1–39. [PubMed: 21118999]
17. Mill P, Lee AW, Fukata Y, Tsutsumi R, Fukata M, Keighren M, Porter RM, McKie L, Smyth I, Jackson IJ. Palmitoylation regulates epidermal homeostasis and hair follicle differentiation. *PLoS Genet*. 2009; 5:e1000748. [PubMed: 19956733]
18. Tsutsumi R, Fukata Y, Noritake J, Iwanaga T, Perez F, Fukata M. Identification of g protein alpha subunit-palmitoylating enzyme. *Mol Cell Biol*. 2009; 29:435–447. [PubMed: 19001095]
19. Mayer TC, Kleiman NJ, Green MC. Depilated (dep), a mutant gene that affects the coat of the mouse and acts in the epidermis. *Genetics*. 1976; 84:59–65. [PubMed: 791749]

20. Swoap SJ, Li C, Wess J, Parsons AD, Williams TD, Overton JM. Vagal tone dominates autonomic control of mouse heart rate at thermoneutrality. *Am J Physiol Heart Circ Physiol.* 2008; 294:H1581–1588. [PubMed: 18245567]
21. Chini B, Parenti M. G-protein-coupled receptors, cholesterol and palmitoylation: Facts about fats. *J Mol Endocrinol.* 2009; 42:371–379. [PubMed: 19131499]
22. Stevens PA, Padiani J, Carrillo JJ, Milligan G. Coordinated agonist regulation of receptor and g protein palmitoylation and functional rescue of palmitoylation-deficient mutants of the g protein g11alpha following fusion to the alpha1b-adrenoreceptor: Palmitoylation of g11alpha is not required for interaction with beta*gamma complex. *J Biol Chem.* 2001; 276:35883–35890. [PubMed: 11461908]
23. Novotny J, Dürchankova D, Ward RJ, Carrillo JJ, Svoboda P, Milligan G. Functional interactions between the alpha1b-adrenoreceptor and galpha11 are compromised by de-palmitoylation of the g protein but not of the receptor. *Cell Signal.* 2006; 18:1244–1251. [PubMed: 16297597]
24. Fukata Y, Iwanaga T, Fukata M. Systematic screening for palmitoyl transferase activity of the dhhc protein family in mammalian cells. *Methods.* 2006; 40:177–182. [PubMed: 17012030]
25. Tanoue A, Nasa Y, Koshimizu T, Shinoura H, Oshikawa S, Kawai T, Sunada S, Takeo S, Tsujimoto G. The alpha(1d)-adrenergic receptor directly regulates arterial blood pressure via vasoconstriction. *J Clin Invest.* 2002; 109:765–775. [PubMed: 11901185]
26. Billaud M, Lohman AW, Straub AC, Looft-Wilson R, Johnstone SR, Araj CA, Best AK, Chekeni FB, Ravichandran KS, Penuela S, Laird DW, Isakson BE. Pannexin1 regulates alpha1-adrenergic receptor-mediated vasoconstriction. *Circ Res.* 2011; 109:80–85. [PubMed: 21546608]
27. Vicentic A, Robeva A, Rogge G, Uberti M, Minneman KP. Biochemistry and pharmacology of epitope-tagged alpha(1)-adrenergic receptor subtypes. *J Pharmacol Exp Ther.* 2002; 302:58–65. [PubMed: 12065700]
28. Ross EM. Protein modification. Palmitoylation in g-protein signaling pathways. *Curr Biol.* 1995; 5:107–109. [PubMed: 7743169]
29. Forrester MT, Hess DT, Thompson JW, Hultman R, Moseley MA, Stamler JS, Casey PJ. Site-specific analysis of protein s-acylation by resin-assisted capture. *J Lipid Res.* 2011; 52:393–398. [PubMed: 21044946]
30. Ren W, Jhala US, Du K. Proteomic analysis of protein palmitoylation in adipocytes. *Adipocyte.* 2013; 2:17–28. [PubMed: 23599907]
31. Huang K, Yanai A, Kang R, Arstikaitis P, Singaraja RR, Metzler M, Mullard A, Haigh B, Gauthier-Campbell C, Gutekunst C-A, Hayden MR, El-Husseini A. Huntingtin-interacting protein hip14 is a palmitoyl transferase involved in palmitoylation and trafficking of multiple neuronal proteins. *Neuron.* 2004; 44:977–986. [PubMed: 15603740]
32. Jensen BC, Swigart PM, Simpson PC. Ten commercial antibodies for alpha-1-adrenergic receptor subtypes are nonspecific. *Naunyn Schmiedebergs Arch Pharmacol.* 2009; 379:409–412. [PubMed: 18989658]
33. Hosoda C, Koshimizu T-a, Tanoue A, Nasa Y, Oikawa R, Tomabechi T, Fukuda S, Shinoura H, Oshikawa S, Takeo S, Kitamura T, Cotecchia S, Tsujimoto G. Two alpha1-adrenergic receptor subtypes regulating the vasopressor response have differential roles in blood pressure regulation. *Mol Pharmacol.* 2005; 67:912–922. [PubMed: 15598970]
34. Chu CP, Kunitake T, Kato K, Watanabe S, Qiu DL, Tanoue A, Kannan H. The alpha 1d-adrenergic receptor modulates cardiovascular and drinking responses to central salt loading in mice. *Neurosci Lett.* 2004; 356:33–36. [PubMed: 14746895]
35. Tanoue A, Koba M, Miyawaki S, Koshimizu TA, Hosoda C, Oshikawa S, Tsujimoto G. Role of the alpha1d-adrenergic receptor in the development of salt-induced hypertension. *Hypertension.* 2002; 40:101–106. [PubMed: 12105146]
36. Yamazaki D, Tabara Y, Kita S, et al. Tric-a channels in vascular smooth muscle contribute to blood pressure maintenance. *Cell Metab.* 2011; 14:231–241. [PubMed: 21803293]
37. Guyton AC. Blood pressure control--special role of the kidneys and body fluids. *Science.* 1991; 252:1813–1816. [PubMed: 2063193]
38. Kopp, UC. Colloquium series on integrated systems physiology: From molecule to function. San Rafael, CA: Morgan & Claypool Life Sciences; 2011. Neural control of renal function; p. 1-96.

39. Methven L, Simpson PC, McGrath JC. Alpha 1a/b-knockout mice explain the native alpha1d-adrenoceptor's role in vasoconstriction and show that its location is independent of the other alpha1-subtypes. *Br J Pharmacol.* 2009; 158:1663–1675. [PubMed: 19888965]
40. Torrecilla I, Tobin AB. Co-ordinated covalent modification of g-protein coupled receptors. *Curr Pharm Des.* 2006; 12:1797–1808. [PubMed: 16712489]
41. Zuckerman DM, Hicks SW, Charron G, Hang HC, Machamer CE. Differential regulation of two palmitoylation sites in the cytoplasmic tail of the beta1-adrenergic receptor. *J Biol Chem.* 2011; 286:19014–19023. [PubMed: 21464135]
42. Li Y, Martin BR, Cravatt BF, Hofmann SL. Dhhc5 palmitoylates flotillin-2 and is rapidly degraded on induction of neuronal differentiation in cultured cells. *J Biol Chem.* 2012; 287:523–530. [PubMed: 22081607]
43. Wan J, Savas JN, Roth AF, Sanders SS, Singaraja RR, Hayden MR, Yates JR 3rd, Davis NG. Tracking brain palmitoylation change: Predominance of glial change in a mouse model of huntington's disease. *Chem Biol.* 2013; 20:1421–1434. [PubMed: 24211138]
44. Ebersole B, Petko J, Levenson R. Bioorthogonal click chemistry to assay mu-opioid receptor palmitoylation using 15-hexadecynoic acid and immunoprecipitation. *Anal Biochem.* 2014; 451:25–27. [PubMed: 24463015]
45. Kokkola T, Kruse C, Roy-Pogodzik EM, Pekkinen J, Bauch C, Honck HH, Hennemann H, Kreienkamp HJ. Somatostatin receptor 5 is palmitoylated by the interacting zdhhc5 palmitoyltransferase. *FEBS Lett.* 2011; 585:2665–2670. [PubMed: 21820437]
46. Milnerwood AJ, Parsons MP, Young FB, Singaraja RR, Franciosi S, Volta M, Bergeron S, Hayden MR, Raymond LA. Memory and synaptic deficits in hip14/dhhc17 knockout mice. *Proc Natl Acad Sci U S A.* 2013; 110:20296–20301. [PubMed: 24277827]
47. Saleem AN, Chen YH, Baek HJ, Hsiao YW, Huang HW, Kao HJ, Liu KM, Shen LF, Song IW, Tu CP, Wu JY, Kikuchi T, Justice MJ, Yen JJ, Chen YT. Mice with alopecia, osteoporosis, and systemic amyloidosis due to mutation in zdhhc13, a gene coding for palmitoyl acyltransferase. *PLoS Genet.* 2010; 6:e1000985. [PubMed: 20548961]
48. Song IW, Li WR, Chen LY, Shen LF, Liu KM, Yen JJ, Chen YJ, Chen YJ, Kraus VB, Wu JY, Lee MT, Chen YT. Palmitoyl acyltransferase, zdhhc13, facilitates bone mass acquisition by regulating postnatal epiphyseal development and endochondral ossification: A mouse model. *PLoS One.* 2014; 9:e92194. [PubMed: 24637783]
49. Mill P, Lee AWS, Fukata Y, Tsutsumi R, Fukata M, Keighren M, Porter RM, McKie L, Smyth I, Jackson IJ. Palmitoylation regulates epidermal homeostasis and hair follicle differentiation. *PLoS Genetics.* 2009; 5:e1000748. [PubMed: 19956733]
50. Fernandez-Hernando C, Fukata M, Bernatchez PN, Fukata Y, Lin MI, Bredt DS, Sessa WC. Identification of golgi-localized acyl transferases that palmitoylate and regulate endothelial nitric oxide synthase. *The Journal of cell biology.* 2006; 174:369–377. [PubMed: 16864653]
51. Huang PL, Huang Z, Mashimo H, Bloch KD, Moskowitz MA, Bevan JA, Fishman MC. Hypertension in mice lacking the gene for endothelial nitric oxide synthase. *Nature.* 1995; 377:239–242. [PubMed: 7545787]
52. Resh MD. Use of analogs and inhibitors to study the functional significance of protein palmitoylation. *Methods.* 2006; 40:191–197. [PubMed: 17012032]
53. Jennings BC, Nadolski MJ, Ling Y, Baker MB, Harrison ML, Deschenes RJ, Linder ME. 2-bromopalmitate and 2-(2-hydroxy-5-nitro-benzylidene)-benzo[b]thiophen-3-one inhibit dhhc-mediated palmitoylation in vitro. *J Lipid Res.* 2009; 50:233–242. [PubMed: 18827284]
54. Martin BR, Wang C, Adibekian A, Tully SE, Cravatt BF. Global profiling of dynamic protein palmitoylation. *Nat Methods.* 2012; 9:84–89. [PubMed: 22056678]
55. Dekker FJ, Rocks O, Vartak N, Menninger S, Hedberg C, Balamurugan R, Wetzel S, Renner S, Gerauer M, Schölermann B, Rusch M, Kramer JW, Rauh D, Coates GW, Brunsveld L, Bastiaens PIH, Waldmann H. Small-molecule inhibition of apt1 affects ras localization and signaling. *Nat Chem Biol.* 2010; 6:449–456. [PubMed: 20418879]

Significance

This study identifies the protein acyl transferase enzyme ZDHHC21 as a novel regulator of alpha1 adrenergic receptor (AR) signaling. Mice with nonfunctional mutants of ZDHHC21 display defective responses to infusions of α 1 AR agonist, as do blood vessels and cells derived from these mice. The mice also display tachycardia and hypotension, despite elevated catecholamine levels. These findings are consistent with defective α 1AR signaling. Further, ZDHHC21 is found to complex with and to increase the attachment of the saturated lipid palmitate to α 1 AR. Since palmitoylation commonly affects the function of G protein coupled receptors like the α 1 AR, these findings suggest a novel molecular mechanism by which α 1 adrenergic signaling, vascular tone and blood pressure may be regulated.

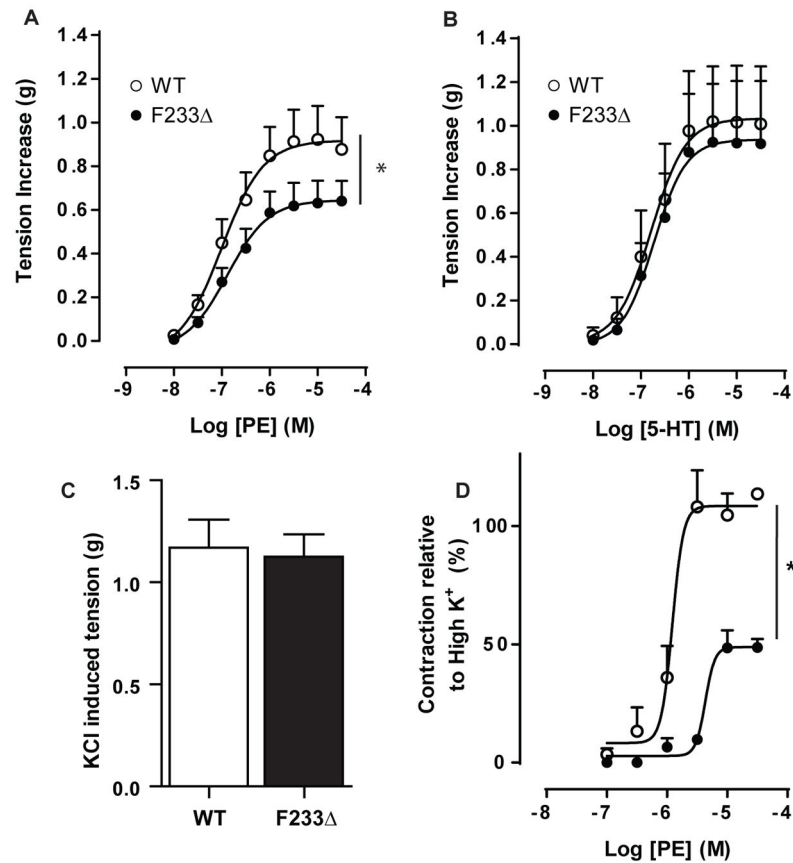


Fig. 1. Myographic measurements on isolated vessels show selective defect in response of F233 vessels to phenylephrine, an α_1 adrenergic receptor agonist

A–C, Wire myography of aortic rings. **A**, **B**, Tension induced in F233 vessels by phenylephrine (PE) is reduced, whereas serotonin (5-HT) induced tension is normal. **C**, Contraction of aortic rings induced by high potassium (60mM), which is receptor independent, is normal. **D**, Pressure myography studies of isolated 3rd order mesenteric arteries shows reduced responsiveness of F233 vessels to phenylephrine. (*, $p < 0.05$ for difference in maximal response as judged by extra sum-of-squares F test. $n = 3$ mice (with 2–3 rings per mouse averaged) for A–C; $n = 3$ mice (with 1–2 vessels per mouse averaged) in D).

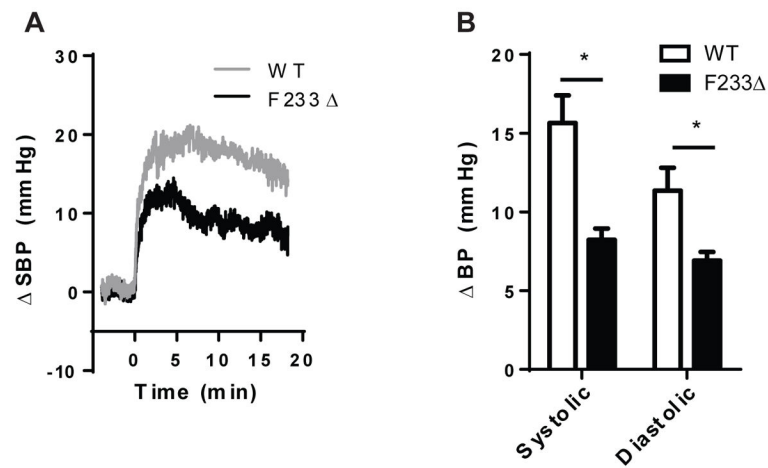


Fig. 2. F233 mice show impaired responses to phenylephrine infusions

A, Phenylephrine was infused intravenously at 30 $\mu\text{g}/\text{kg}/\text{min}$ starting at time zero while hemodynamics were monitored via an intraarterial catheter in anesthetized mice. Changes in SBP over time are shown for WT and F233 mice from a representative experiment. **B**, Mean plateau changes in SBP and DBP after 15 min of phenylephrine infusion are plotted; $n=6$. *, $p < 0.05$ by two-tailed t test.

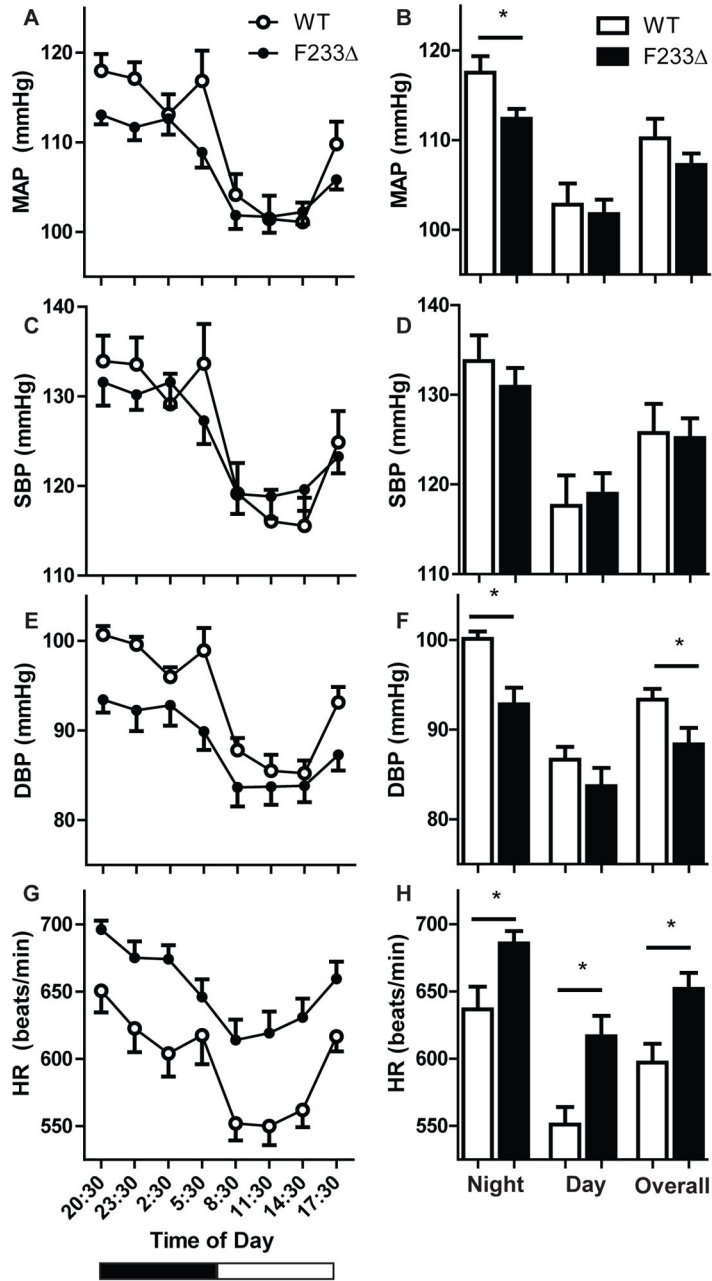


Fig. 3. F233 mice are tachycardic and hypotensive

Blood pressure (BP) and heart rates (HR) were determined in unrestrained, unanesthetized mice using an implantable telemetry system. **A, C, E, G**, 24 hours of data are shown at times indicated on a 24 hour scale; night is indicated by a black bar and day by white. Data shown at each time point represent 3 hour rolling averages of data sampled once each minute. Further, data at each time point are averaged from 3 consecutive days of monitoring for each mouse. MAP, mean arterial pressure; SBP, systolic blood pressure; DBP, diastolic blood pressure. The data show decreased MAP and DBP during the night in F233 mice. In addition, the F233 mice are tachycardic at all time points relative to WT. **B, D, F, H**, Mean values for

MAP and HR were calculated at peak night (19:00–1:00) and day (7:00–13:00) times and displayed as bar graphs. *, $p < 0.05$ by two tailed t test, $n = 7$ mice per group.

Author Manuscript

Author Manuscript

Author Manuscript

Author Manuscript

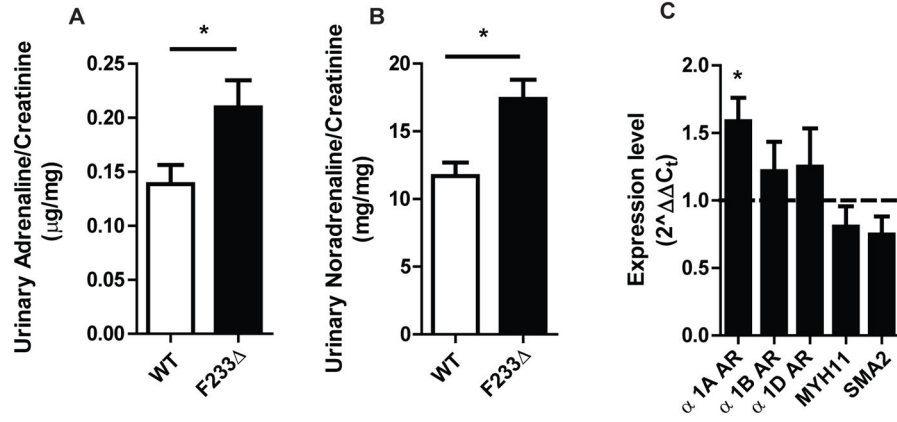


Fig. 4. Altered levels of catecholamines and α_1 adrenergic receptor transcripts in F233 mice
A, B. Ratios of urinary adrenaline and noradrenaline to creatinine were elevated in F233 mice. $n=9-14$ mice per group. *, $p < 0.05$ by two tailed unpaired t test. **C.** Aortae from F233 mice displayed increased expression of α_1 adrenergic receptor 1A gene but not genes encoding the structural proteins MYH11 or SMA2 as judged by qPCR. *, $p < 0.05$ for F233 compared to WT.

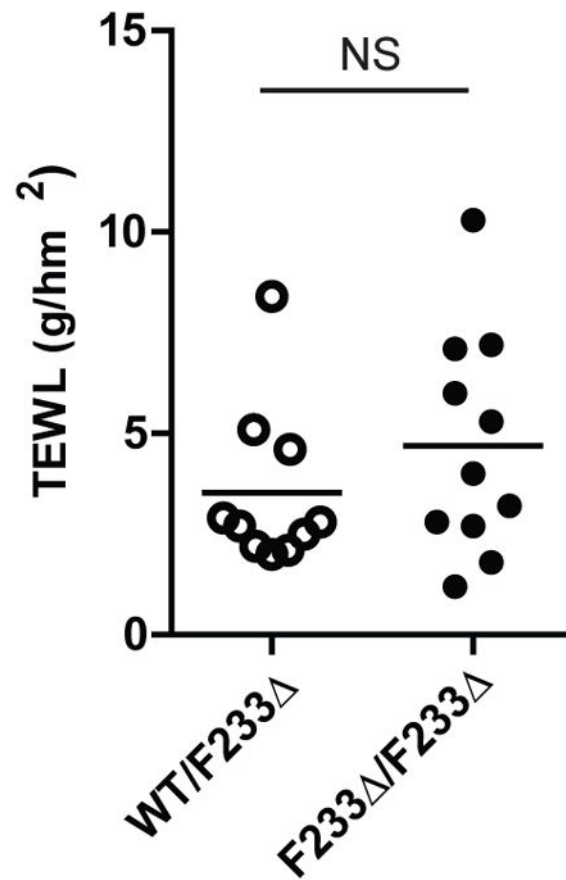


Fig. 5. F233 Δ mice do not lose fluid via skin

Transepidermal water losses (TEWL) were measured to determine whether fluid losses might occur via the skin, given the abnormal fur and skin in F233 Δ mice¹⁷. TEWL in the F233 Δ mice was not significantly different from that in the WT mice ($p = 0.29$ by two tailed t test).

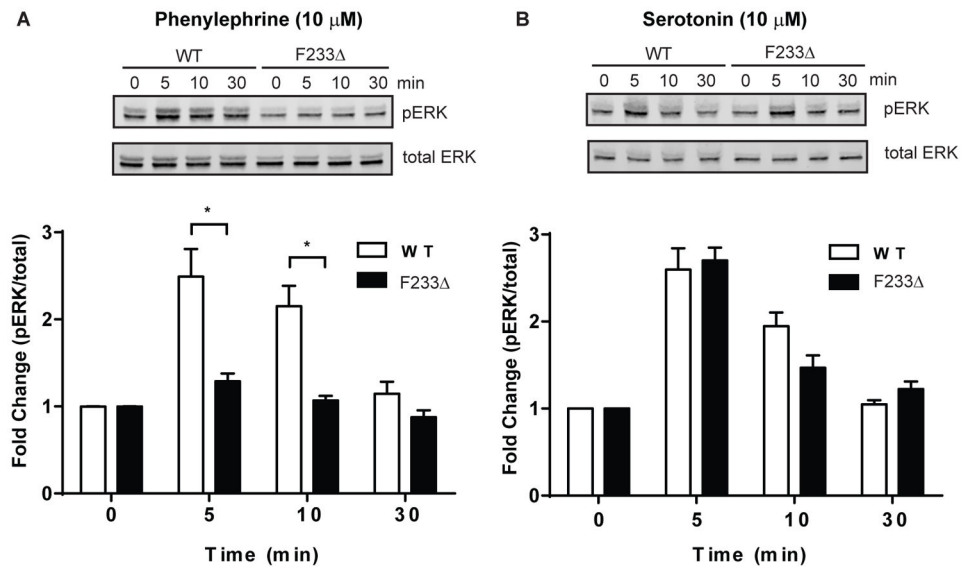


Fig. 6. Phenylephrine signaling is impaired in embryonic fibroblasts from F233 mice
 The phosphorylation of ERK was measured by Western blot at indicated time points after exposure to 10 μ M phenylephrine (A) or 10 μ M serotonin (B). Phospho-ERK signal was normalized by total ERK, and adjusted to 1 at time zero. Phenylephrine signaling was impaired but serotonin signaling was normal. *, $p < 0.05$ by 2-way ANOVA with Bonferroni post-test; $n = 7$.

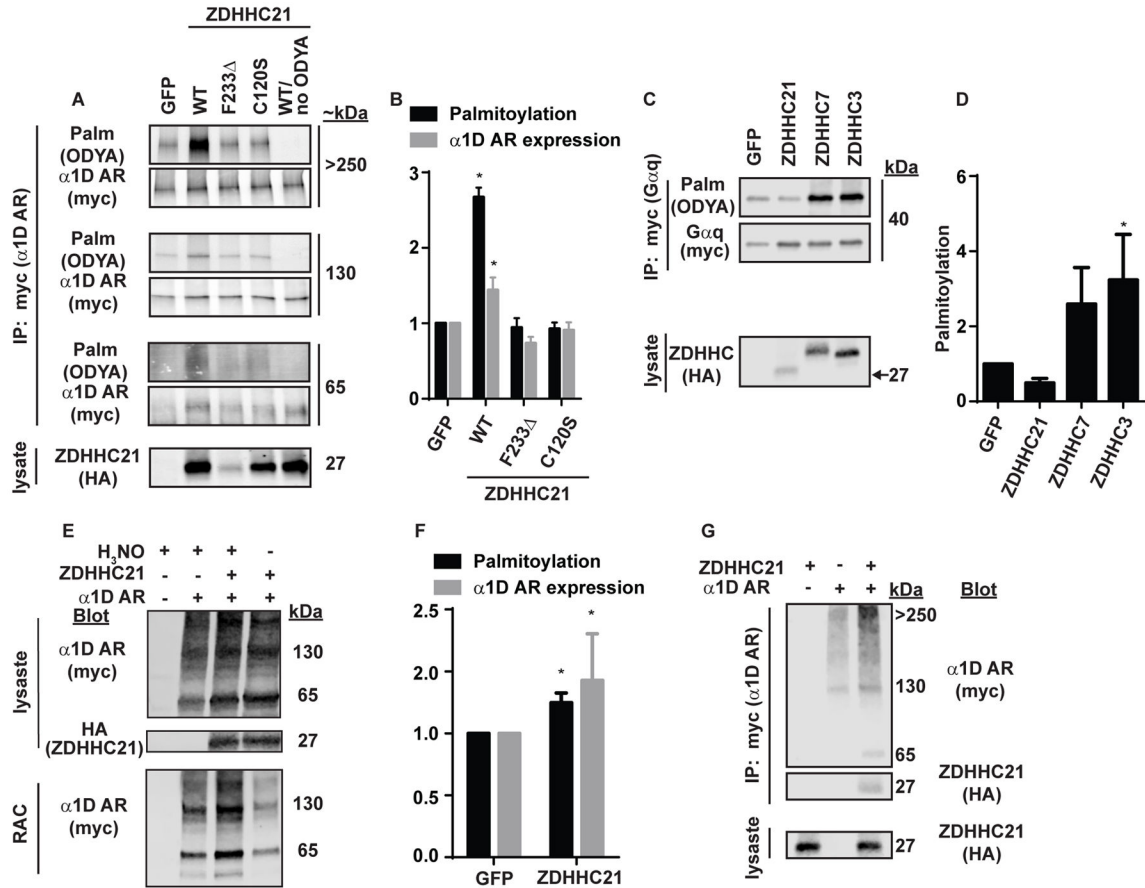


Fig. 7. ZDHHC21 palmitoylates α 1D AR but not $G\alpha q$

A. α 1D AR (myc-tagged) was expressed in HEK293 cells along with GFP (control), WT ZDHHC21, or nonfunctional ZDHHC21 mutants (HA-tagged). The degree of palmitoylation was determined by metabolic labeling with the palmitate analog ODYA, followed by immunoprecipitation of α 1D AR, and click chemistry to attach a fluorophore to incorporated ODYA. The intensity of the ODYA signal was normalized to the total amount of α 1D AR as determined by Western blot. The α 1D AR tends to aggregate when expressed in HEK293 cells, and can be detected as monomers, dimers, and higher order aggregates at mol wt of ~65, ~130, and >250kDa. **B.** Quantitation of palmitoylation (i.e., normalized ODYA incorporation) and total α 1D AR expression, $n=3$, *, $p<0.05$ compared to GFP, by one-way ANOVA with Dunnett's post test. **C.** ZDHHC21 does not palmitoylate $G\alpha q$, whereas ZDHHC3 does. **D.** Quantitation of $G\alpha q$ palmitoylation. $n=3$, *, $p<0.05$ compared to GFP, by one-way ANOVA with Dunnett's post test. **E.** ZDHHC21 increases α 1D AR palmitoylation as judge by acyl-RAC methodology. Palmitoylated alpha1D AR is isolated in presence, but not absence of hydroxylamine (H_3NO). **F.** Quantitation of palmitoylation (normalized to total expression) and total expression of α 1D AR; both are increased by ZDHHC21. $n=5$ *, $p<0.05$ compared to GFP by two tailed t test. **G.** ZDHHC21 can be coimmunoprecipitated by α 1D AR, suggesting the two proteins interact in a molecular complex. The data are representative of three experiments.

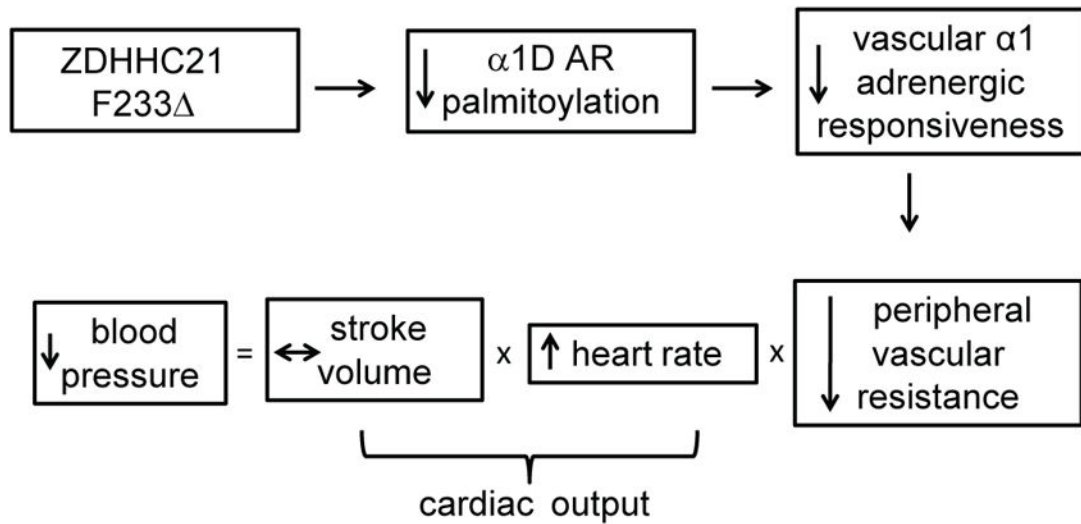


Fig. 8. Proposed model of disturbed physiology in F233 mice

Mutation of ZDHHC21 causes decreased α 1D AR function (possibly due to reduced vascular α 1D AR palmitoylation) which results in diminished peripheral vascular resistance (PVR). The reduced PVR manifests as reduced BP as observed in the telemetry studies, although the reduction is mitigated by increased HR (Fig. 3).

Table 1**Echocardiographic parameters**

Anesthetized mice were analyzed with a Vevo 2100 ultrasound system. Parameters shown were derived by tracing the images of the left ventricle at systole and diastole. F233 mice showed no significant difference from WT in any of the parameters shown; n= 9, p>0.05 for all comparisons by unpaired two-tailed t test.

	WT	F233
Stroke Vol, μL	41.7 \pm 1.2	40.8 \pm 2.1
Ejection Fraction, %	53 \pm 3	55 \pm 2
Left Ventricular (LV) Mass, mg	114.0 \pm 4.7	111.5 \pm 8.2
LV volume, μL (diastole)	79.4 \pm 2.8	76.3 \pm 5.5
LV volume, μL (systole)	38.1 \pm 3.2	35.6 \pm 3.9

Author Manuscript

Author Manuscript

Author Manuscript

Author Manuscript

Table 2**Blood analyses**

Blood was collected via retro-orbital bleeds from anesthetized mice and analyzed using an iStat instrument and EC8+ cartridges. Data are the mean \pm SEM; n=11 for each group. P values are calculated by two tailed unpaired Student's t test.

	WT	F233	p
Na, mEq/L	145.0 \pm 3.0	145.5 \pm 1.3	0.695
K, mEq/L	4.3 \pm 0.8	4.5 \pm 0.5	0.309
Cl, mEq/L	113.9 \pm 1.9	110.5 \pm 1.5	0.003
HCO ₃ , mEq/L	22.8 \pm 1.9	26.5 \pm 1.9	0.001
BUN, mg/dL	23.1 \pm 3.9	19.0 \pm 1.3	0.116
Glu, mg/dL	206.5 \pm 24.8	204.9 \pm 36.5	0.911
Hct, %	42.5 \pm 2.3	43.3 \pm 1.7	0.496
pH	7.2 \pm 0.1	7.2 \pm 0.1	0.426
pCO ₂ , mmHg	59.4 \pm 9.6	65.1 \pm 6.0	0.096
AG	12.5 \pm 2.5	13.0 \pm 2.2	0.630
Hgb, g/dL	14.5 \pm 0.8	14.7 \pm 0.6	0.534